Springer

KSME

Journal of Mechanical Science and Technology 33 (8) (2019) 3851~3858
www.springerlink.com/content/1738-494x(Print)/1976-3824(Online)
DOI 10.1007/s12206-019-0728-9

Numerical analysis and simulation of an impulse driven piezoelectric needle-free jet injector †

Mojiz Abbas Trimzi[1,2], Young-Bog Ham[1,2,*], Byeung-Cheol An[1,2], Jung-Ho Park[2] and So-Nam Yun[1,2]

[1]*Department of Plant System & Machinery, University of Science & Technology, Daejeon, Korea*
[2]*Department of Thermal Systems, Korea Institute of Machinery & Materials, Daejeon, Korea*

(Manuscript Received August 22, 2018; Revised March 21, 2019; Accepted July 4, 2019)

Abstract

Transdermal drug delivery using needle free jet injections entails ejection of a liquid drug through a fine nozzle at elevated pressure, thus generating a narrow high-velocity fluid jet readily penetrable into skin and tissue. The idea of a simple and compact piezoelectric powered needle free injector (NFI) is introduced in this article, which offers electric control of injection volume in microliters. An impulse of up to 3500 N-s or more is generated by the multilayer piezoelectric actuator to drive the needle-free injector. The governing equations for the force and mass balance over the syringe plunger were derived to represent the driving mechanism for a compact needle-free injector. Furthermore, simulation was carried out to witness the effect of variation in parameters like impulse force, nozzle diameter and nozzle length on the injection dynamics, and the results prove the dependence of injection characteristics on aforementioned parameters, respectively. Finally, the specifications for fabrication of 10 μl volume delivering piezoelectric-impulse driven needle-free injector were obtained through analysis of multiple simulation results.

Keywords: Multilayer piezoelectric actuator; Mechanical impulse; SimulationX; Liquid jet injection; Compact injector

1. Introduction

Rapid discovery and development of drugs with the passage of time has ensured the cure of many diseases, but effective drug delivery has been an under-explored area of research. Transdermal drug delivery represents an attractive alternative to the most commonly adopted oral delivery of drugs and is expected to offer an alternative to hypodermic injection, too [1-4]. Drugs with large molecules like most of the vaccines are injected through needles as they cannot be administered orally or absorbed by skin [5]. The need for trained nurses, needle phobia, and inadequate delivery of improper volumes of drugs has catalyzed the research to find drug delivery alternatives which offer simple and painless drug administration [6]. Various kinds of micro-needles are being developed for advancement in drug delivery through the skin, but there are challenges to delivering high molecular weight drugs [7-10]. Chemical penetration catalyzers, skin permeabilization and jet injectors as well are the recently studied areas for transdermal drug delivery [11-16]. The non-parental transdermal delivery of biopharmaceuticals is widely studied field these days, yet there are fierce complications for penetration of drug molecules into stratum corneum [17, 18]. Jet injectors, for parental administration of drug with high velocity into skin, have been studied in the past seven decades [19, 20]. Some drawbacks of jet injectors include splash-back of drug, unreliable drug depth, unpredicted dose delivery, painful bruises and bleeding [21-24]. The causes of this unreliability include unsuitability of available devices to tackle variation in skin thickness, large drug volumes, and large nozzle sizes, which is also the cause of splash-back and pain caused by jet injectors [21, 23]. These limitations of jet injectors are addressed in the recent research. Jet injectors are now being used for transdermal gene delivery by stratum corneum disruption and intra-cavernosal therapies as well [25, 26].

In this paper, idea of electrically controlled drug delivery using impulse type jet injector is proposed for improved and consistent microliter drug administration by lesser pain. The proposed design of an impulse type needle free injector is powered by the instantaneous expansion of multilayered piezoelectric actuator to displace fluid through a fine sized nozzle. Conventional spring powered, compressed gas powered, and bubble driven injection device do not offer compact and silent operation with accurate control of injection speed [27-29]. In addition, drug pressure, and nozzle size have not been addressed previously. Previous studies have shown that piezo-

*Corresponding author. Tel.: +82 42 868 7157, Fax.: +82 42 868 7335
E-mail address: hyb665@kimm.re.kr
† This paper was presented at ETME 2018, Ramada Plaza Jeju Hotel, Jeju, Korea, August 19-22, 2018. Recommended by Guest Editor Maenghyo Cho.

electric actuators can be used to achieve high velocity fluid jets for penetration and delivery of insulin into animal skin [30, 31]. The recent multilayered piezoelectric (PZT) actuators have lower power consumption, fast expansion, no wear and tear, vacuum and clean room compatibility, and exhibit better conversion efficiency of electrical to mechanical energy [32-37]. They can generate blocking force ranging from 300 N to 14000 N with maximum strokes varying from 13/9 μm to 270/200 μm by application of -30 V~150 V potential difference [38]. If necessary, the scope for applications of piezoelectric actuators is enhanced by using displacement amplification mechanisms to enhance the stroke length of piezostack actuator, which include lever-type, moonie-type, rainbow-type, cymbal-type, ellipse-type, rhombus-type, bridge-type, rhombus with hinges, compound bridge-type, and three-dimensional displacement amplification mechanisms [39-45]. The displacement amplification enhances the displacement up to 12 times, but it reduces the blocking force proportional to the displacement amplified [46]. The conventionally available multilayered piezoelectric actuator, without displacement amplification accessories, is considered as a power source for impulse type needle free injector [47, 48].

In this study, governing equations for numerical analysis of a compact, piezoelectric impulse driven needle free jet injector were derived. Instead of solving the equations repeatedly by changing minor parameters in a conventional way, model simulations were carried out to study the effect of force generated by multilayered piezoelectric actuator on pressure drop across the nozzle, which had not been addressed previously. The approach of utilizing simulation tool instead of cumbersome numerical solutions was adopted. Furthermore, the effect of variation of nozzle length and nozzle diameter, by keeping the piezostack force constant, on injection dynamics was analyzed. The piezostack force, which accelerates the plunger, was varied from 1000 N to 3500 N to observe its effect on pressurization of drug volume, which is the core parameter for the high velocity jet propagation out of a fine sized nozzle. The simulation model verifies the feasibility of utilizing the impulse mechanism to power the needle free injector and potential possibility of realization of piezo-stack impulse mechanism in needle free drug delivery device. The simulation results emphasize that the injection characteristics strongly depend on force generated by piezostack actuator, diameter of nozzle and length of nozzle, respectively.

2. Numerical analysis and modeling

2.1 Conceptual design

The proposed prototype of needle free jet injector to be designed is composed of a metal frame, the upside of which provides stiff support to the rigid end of piezoelectric actuator. The position of actuator can be adjusted by upper adjust-nut. The metal frame is connected to the syringe plunger through screw threads, and the drug supply line equipped with unidirectional check valve opens in the plunger cavity, as shown in Fig. 1.

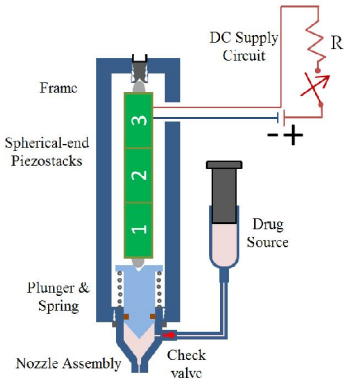

Fig. 1. Piezoelectric impulse needle free jet injector assembly.

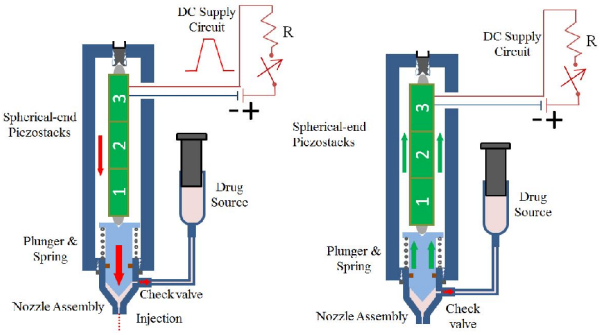

(a) Piezostacks in excited state (b) Returning to neutral state

Fig. 2. Impulse NFI: (a) Excited state; (b) neutral state.

2.2 Working mechanism

The injector is powered by DC supply line through the frame. Upon application of a voltage, the piezoelectric actuator excites, which in turn induces an instantaneous impulse to the syringe plunger. The plunger accelerates downwards by increasing the compression in the spring; as a result, the drug volume inside the plunger cavity gets pressurized causing a high pressure jet of drug from the nozzle at the bottom of the injector. When the DC supply is disconnected, the piezostack contracts and the spring force overcomes the accumulative mass of piezostack and syringe plunger by moving the plunger upwards. This phenomenon can be controlled by controlling the DC supply.

Fig. 2 represents the working principle of the piezoelectric impulse needle-free injector.

2.3 Mathematical model

The mechanism of impulse needle-free injector can be represented mathematically by derivation of governing equations considering the aforementioned working principle of needle free injector. The length of piezo-stack actuator in neutral state is L_o. When electric voltage is applied, the piezostack expands

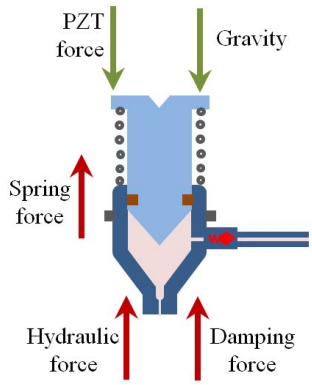

Fig. 3. Force balance over syringe plunger.

and its length increases proportional to the applied potential difference. The piezostack length is represented as $L_{PZT} = L_o + f(V)$. If x represents the expansion in length of piezostack, then x is the function of applied voltage $[x = f(V)]$. Thus, the relationship representing length of PZT stack at any instant is given below.

$$L_{PZT} = L_o + x. \tag{1}$$

Similarly, the syringe plunger is considered in mechanical contact with the piezostack actuator. The return spring has free length of L_o'. x_o is the pre-compression in the spring, which is considered to reduce the dead band. x_{PL} is further compression in the spring caused by expansion of piezostack actuator. The total compression in the spring is expressed as $x_s = x_o + x_{PL}$. The spring length further decreases by expansion of piezostack actuator. The relationship to represent the instantaneous length of spring is expressed as follows.

$$L_{SPR} = L_o' - x_o - x_{PL}\,. \tag{2}$$

Eqs. (1) and (2) represent the geometrical consideration for expansion of piezostack with respect to contraction in spring and vice versa.

The force balance over the syringe plunger suggests that the sum of all the forces acting on the syringe plunger is equal to the mass times acceleration of the syringe plunger, which can be expressed as $(\sum F)_{PL} = m_{PL}.\ddot{x}_{PL} = 0$. If the needle-free injector assembly is considered to be positioned downwards against the gravity, then the forces acting on syringe plunger include PZT stack force (F_{PZT}), gravity force ($m_{PL}g$), spring force [$k(x_{PL}+x_o)$], hydraulic force [$(\pi/4)D_P^2.P$] and damping force ($C_f\dot{x}_{PL}$) as described in Fig. 3.

The gravity and piezostack force are considered to be positive; thus the opposing forces are taken as negative. The expression for force balance over the syringe plunger is given in Eq. (3).

$$F_{PZT} + m_{PL}g - k(x_{PL}+x_o) - \left[\frac{\pi}{4}D_P^2.P\right] - C_f\dot{x}_{PL} = m_{PL}\ddot{x}_{PL}\,. \tag{3}$$

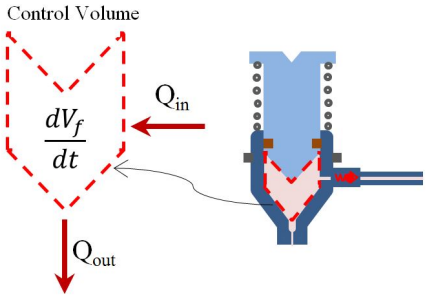

Fig. 4. Control volume consideration for pressure evaluation in plunger cavity.

Manipulation of force balance Eq. (3) gives pressure build-up across the nozzle as shown in Eq. (4).

$$P = \frac{F_{PZT} + m_{PL}g - k(x_{PL}+x_o) - C_f\dot{x}_{PL} = m_{PL}\ddot{x}_{PL}}{(\pi/4).D_P^2}\,. \tag{4}$$

The syringe plunger movement causes displacement in volume of fluid below plunger. The expression for volume of the fluid displaced by the plunger is represented by Eq. (5).

$$\frac{dV_f}{dt} = \left(\frac{\pi}{4}D_{PL}^2\right)\cdot\dot{x}\,. \tag{5}$$

Similarly, the fluid jet injected out of the nozzle can be expressed as Eq. (6).

$$Q_{OUT} = \left(\frac{\pi}{4}D_N^2\right)\cdot v_f\,. \tag{6}$$

Consideration of liquid chamber of needle-free injector as a control volume results in the expression for drug flow out of nozzle, which is expressed as Eq. (7). Fig. 4 represents the control volume under consideration.

$$\left(\frac{\pi}{4}D_{PL}^2\right)\cdot\dot{x} = \frac{V}{\beta}\frac{dP}{dt}\left(\frac{\pi}{4}D_N^2\right)\cdot v_f\,. \tag{7}$$

The expression for velocity of fluid out of nozzle can be derived from Bernoulli's Eq. (8).

$$P_1 + \frac{1}{2}\rho v_1^2 + \rho g z_1 = P_2 + \frac{1}{2}\rho v_2^2 + \rho g z_2\,. \tag{8}$$

The height difference (z_2- z_1) in this case is negligible and v_1 is zero; thus Eq. (8) reduces to Eq. (9).

$$P = P_{ATM} + \frac{1}{2}\rho v_2^2\,. \tag{9}$$

The expression for jet velocity out of nozzle Eq. (10) can be substituted in Eq. (7) to get final expression Eq. (11) for the

velocity of plunger, which causes jet injection out of nozzle.

$$v_f = \sqrt{\frac{2(P-P_{ATM})}{\rho}} \tag{10}$$

$$\left(\frac{\pi}{4}D_{PL}^{\ 2}\right)\cdot\dot{x} = \frac{V}{\beta}\frac{dP}{dt}\left(\frac{\pi}{4}D_N^{\ 2}\right)\sqrt{\frac{2(P-P_{ATM})}{\rho}}\,. \tag{11}$$

Eq. (11) is rearranged in terms of plunger velocity.

$$\dot{x} = \frac{\frac{V}{\beta}\frac{dP}{dt}\left(\frac{\pi}{4}D_N^{\ 2}\right)\sqrt{\frac{2(P-P_{ATM})}{\rho}}}{\left(\frac{\pi}{4}D_{PL}^{\ 2}\right)}\,. \tag{12}$$

The system of above derived twelve equations can be solved for the forces acting on plunger, velocity and acceleration of syringe plunger, pressure build up in the drug chamber, and velocity of drug ejected out of nozzle. Instead of repeatedly solving the above equations to get results necessary for specification design of impulse jet injector, a simulation model for the impulse needle free injector was developed. Using the theory behind the derived equations, a simulation model for impulse needle free jet injector was used to carry out multiple simulations for derivation of useful results to derive design specification of proposed needle free injector.

2.4 Simulation modeling

The simulation of the impulse type needle free injector is carried out using a simulation tool called SimulationX® 3.7 software by ESI ITI GmbH [34, 49]. The simulation model is developed by division of needle-free injector assembly into three parts in accordance with the mathematical model. The first part represents piezostack force generation mechanism, the second portion represents movement of syringe plunger due to mechanical impulse, and the third part represents drug dynamics due to pressure generated in plunger cavity and nozzle.

The spring mass damper in the second part helps to control the chaotic friction-induced vibration and ensures the stability of impulse propagation [50]. The parameters considered during simulation are in Table 1. The linear multi-step method is introduced to solve the first-order ordinary differential equations and a fifth-order backward differentiation formula (5th BDF) as shown in Eq. (13) is employed in the linear multistep method.

$$\begin{aligned} y_{n+6} - \frac{360}{147}y_{n+5} + \frac{450}{147}y_{n+4} - \frac{400}{147}y_{n+3} + \frac{225}{147}y_{n+2} \\ - \frac{72}{147}y_{n+1} + \frac{10}{147}y_n \;=\; \frac{60}{147}hf(t_{n+6}, y_{n+6})\,. \end{aligned} \tag{13}$$

After linearization, the results are analyzed by a sparse matrix solver. The minimum step size is 0.1 ns and the minimum output size is 0.1 μs. The default value of damping coefficient is used for the fluid considered as drug, which is built-in fluid HLP46 in SimulationX. The fluid properties like bulk modulus and density are defined and temperature is set to be 25 °C [29]. The simulation model is shown in Fig. 5.

Table 1. Parameters considered for simulation of NFI.

Components	Parameter	Unit
PZT part	PZT force= 3500; 1000	[N]
	Piezo-stack mass= 50	[g]
Plunger part	Spring stiffness = 100000	[N/m]
	Plunger mass= 20	[g]
Plunger cavity	Diameter = 10 - 20	[mm]
	Plunger stroke = 0.05 - 2.0	[mm]
	Dead volume = 0.5	[mm³]
Nozzle part	Drug volume = 5 - 20	[mm³]
	Nozzle length = 0.01 -0.5	[mm]
	Nozzle diameter = 0.01 - 0.3	[mm]

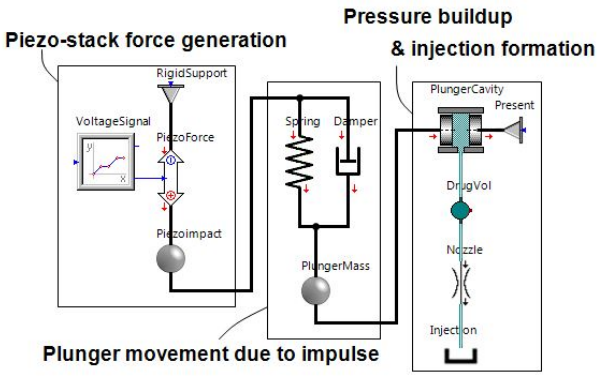

Fig. 5. Simulation model for proposed impulse needle free injector.

The purpose of simulation is to observe the effect of various parameters like PZT force, nozzle length, and nozzle diameter, on the injection dynamics. The flow rate across the nozzle Q_{out} is calculated by Eq. (14). The meter-in pressure drop inside nozzle is also considered, whereas the value of constant K depends on the flow rate.

$$Q_{out} = \frac{2.D_N.A_N}{C_f.L_N.\upsilon.\rho}.\frac{1}{1+K}.P_{ab}\,. \tag{14}$$

Similarly, mass flow rate (*m dot* in *grams per second*) is resulted by product of density and volume flow as shown in Eq. (15)

$$mdot = \rho.Q_{OUT}\,. \tag{15}$$

3. Results and discussion

3.1 Influence of design parameters on injection kinetics

The simulation results are obtained by gradual variation of

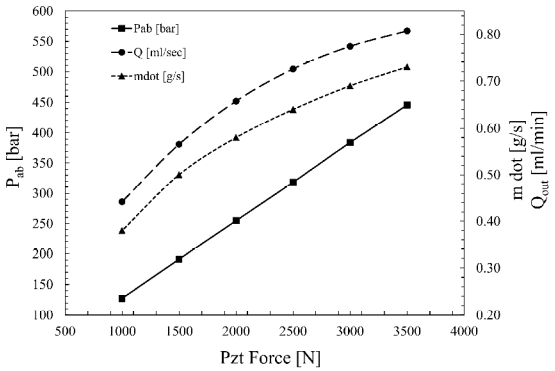

Fig. 6. Effect of force variation on pressure drop across nozzle, injection volume, and mass flow rate.

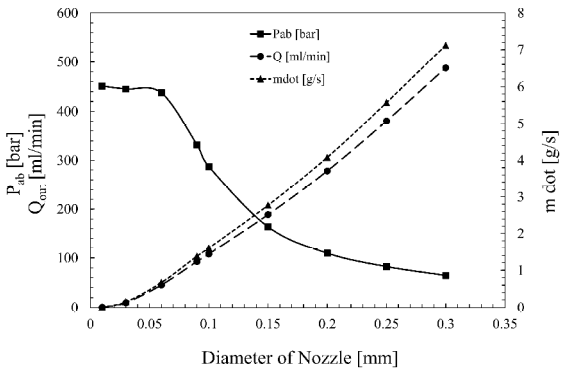

Fig. 7. Influence of nozzle diameter variation on pressure drop across nozzle, injection volume, and mass flow rate.

the force from 1000 N to 3500 N, diameter of nozzle from 0.01 mm to 0.3 mm, and length of nozzle from 0.05 mm to 0.5 mm. The obtained results are then analyzed and conclusions are derived from results. The final simulation delivers the optimum parameters for fabrication of impulse type needle free injector to deliver 10 μl injection volume per shot.

3.1.1 Influence of F_{PZT} on injection dynamics

The first case is the consideration of variation in piezostack force applied in the form of impulse to the syringe plunger. The applied voltage controls the expansion of multilayered piezostack precisely; therefore, the input force over the syringe plunger is electrically controlled by applied voltage [32]. Graphs are plotted (Fig. 6) to witness the effect of variation in PZT force on pressure built-up in drug chamber, injection volume per unit time out of nozzle, and mass of drug injected out of nozzle per unit time. The gradual increase in applied impulse force results in increased pressure difference across the nozzle causing increase in injection volume flow and mass flow and vice versa.

The piezostack force is varied from 1000 N to 3500 N with a difference of 500 N without reaching maximum blocking force limit of piezostack actuator. The gradual decrease in instantaneous impulse force results in considerable reduction in pressure across the nozzle, volume flow rate, and mass flow rate out of nozzle (Fig. 6). The force applied by piezostack, accelerates the syringe plunger, which controls the injection dynamics.

3.1.2 Effect of nozzle diameter (D_N) on injection dynamics

Effect of variation in nozzle diameter on pressure drop across nozzle, volumetric flow rate, and mass flow rate out of nozzle is plotted (Fig. 7). The nozzle diameter is varied by keeping the nozzle length and other parameters constant. The diameter of nozzle is a fundamental parameter to be considered for successful design of needle free injector. Reduction in diameter of nozzle enhances pressure buildup in plunger cavity, whereas decreases the drug volume injected out of nozzle. The reason for considering 0.01 mm to 0.3 mm diameter of nozzle is to keep the size of nozzle practically fabricate-able

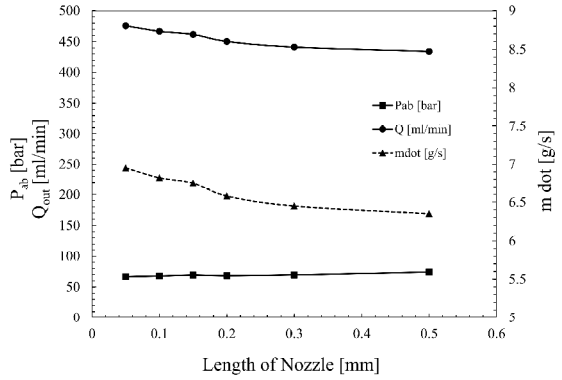

Fig. 8. Effect of nozzle length variation on pressure drop across nozzle, injection volume, and mass flow rate.

for realization of needle-free injector.

The nozzle diameter is a very significant parameter for needle-free injectors. The minor variation in diameter of nozzle can result is undesired drug volume delivery, which should be avoided. For this reason, nine different nozzle diameters were considered, ranging from 0.01 mm to 0.30 mm, to observe the effect of nozzle diameter on pressure drop across the nozzle (Fig. 7).

The length of nozzle (0.01 mm) and input force (3500 N) were kept constant during simulation. The results indicate that a gradual increase in nozzle diameter increases the drug volume injected out of the nozzle. Therefore, reduction in pressure buildup across a nozzle results in weak jet propagation, which finally results in splash back with zero skin penetration capability.

3.1.3 Effect of nozzle length (L_N) on injection dynamics

Influence of nozzle length variation on pressure built-up in drug chamber, volume flow rate out of nozzle, and mass flow rate of drug injected out of nozzle was obtained through simulation. Fig. 8 shows the simulation results for six nozzle lengths from 0.50 mm to 0.05 mm, respectively.

Fig. 8 helps one to observe the effect of nozzle length variation on volume and mass flow rate, out of nozzle. Pressure drop across a nozzle increases with increase in nozzle length

Table 2. Optimum specifications for needle free injector design.

Parameters	Value
Nozzle diameter	100 μm
Nozzle length	100 μm
Piezostack blocking force	3500 N
Plunger cavity diameter	15.6 mm
Plunger stroke	55 μm
Dead volume	5 mm^3

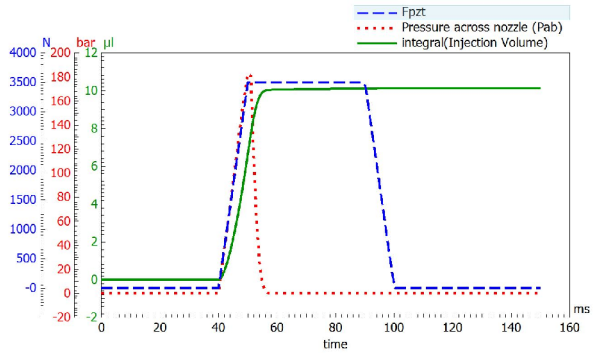

Fig. 9. Simulation results for optimized 10 μl delivery NFI.

as the friction across the walls of nozzle is increased. The opposite phenomenon happens by increasing the nozzle diameter. The nozzle length and nozzle diameter are inversely related to each other. During simulation, nozzle diameter (0.30 mm), applied force (3500 N) and other parameters were kept constant. The trend of inverse dependency of injection volume on nozzle length is very minor because the value of nozzle diameter was kept bigger (D_N: 0.30 mm) to keep the simulated nozzle geometry practically possible for fabrication.

3.2 Optimum parameters for NFI design

Multiple simulations were carried out by changing various parameters to observe their influence on injection dynamics. In the end, some parameters were selected from literature, whereas others were selected by hit and trial method. Table 2 represents the optimum parameters for design of piezoelectric impulse driven needle-free injector for delivery of 10 μl injection volume per shot. As the piezoelectric actuators generate very short displacements in terms of tens of micrometers over application of 150 V, the small volume delivery in terms of microliters is possible at elevated pressure or 120 bar and more, which ensures the penetration of fine liquid jet into skin.

The simulation result in Fig. 9 represents the volume and pressure built-up profile with respect to applied piezoelectric force. The piezoelectric actuator's blocking force and stroke length are taken from commercial PIEZOMECHANIK catalogue [38]. The other parameters are obtained through simulation to get 10 μl injection volume. The instantaneous pressure build-up of 182.58 bar is generated due to instantaneous mechanical impulse transfer by piezostack actuation. From pressure build-up to pressure drop, 10 μl of fluid volume is jetted across the nozzle. This whole phenomenon takes place in less than 20 milliseconds. The process can be repeated to get multiple shots in very short time, as multilayer piezoelectric actuators offer high frequencies up to 20 kHz.

4. Conclusions

The impulse mechanism for needle-free drug delivery using piezostack actuated jet injector is proposed. A numerical analysis for modeling of needle free injector was carried out. Simulations were performed to observe the effect of applied force and nozzle geometry on the built-up pressure, injection mass and volume flow through nozzle. Following conclusions were obtained:

- The expansion of the piezo-stack is a function of applied voltage. Thus, the injection volume can be electronically controlled by controlling the applied voltage. The voltage applied to the piezo-stack directly affects the phenomenon of jet formation from a nozzle.

- The nozzle length and diameter are inversely related. The fabrication of nozzles with less than 100 μm is practically challenging, whereas nozzles with diameters exceeding 100 μm result in splash back or no penetration of jet into skin due to low pressure jetting. The optimum size for nozzle diameter (100 μm) and nozzle length (100 μm) is obtained through simulation.

- Finally, simulation for 10 μl jet injector design was conducted and the crucial parameters for fabrication of jet injector were evaluated. The plunger cavity diameter was optimized to be 15.6 mm due to limited (55 μm) stroke of piezostack actuators.

Acknowledgments

The authors would like to acknowledge the research project support by the UST Young Scientist Research Project (YSRP) of University of Science and Technology (UST), South Korea (Grant No. GM4260).

Nomenclature

L_{PZT} : Piezostack expansion
L_{SPR} : Compression in spring
F_{PZT} : Force applied by piezo-stack
D_{PL} : Diameter of plunger
$x = f(V)$: Displacement of Pzt stack
$\dot{x}_{PL}$: Velocity of plunger
m_{PL} : Mass of plunger
$\ddot{x}_{PL}$: Acceleration of plunger
V_f : Plunger cavity
ρ : Density of HLP46 fluid
β : Bulk modulus of HLP46 fluid
D_N : Diameter of nozzle
v_f : Velocity of fluid passing through nozzle

Q_{out} : Drug volume displaced out of nozzle
mdot : Mass flow out of nozzle
dP/dt : Change in pressure with time
P_{ab} : Pressure drop across nozzle
C_f : Friction coefficient
A_N : Cross-section area of nozzle
L_N : Length of nozzle
ν : Kinematic viscosity

References

[1] R. H. Guy et al., *Transdermal Drug Delivery*, Marcel Dekker, New York (2002).

[2] A. C. Williams et al., *Transdermal and Topical Drug Delivery: From Theory to Clinical Practice*, Pharmaceutical Press, London (2003).

[3] M. R. Prausnitz et al., Transdermal drug delivery, *Nat. Biotechnol.*, 26 (2008) 1261-1268.

[4] R. L. Bronaugh et al., *Percutaneous Absorption: Mechanisms, Methodology, Drug Delivery*, Edn. 4, Marcel Dekker, New York (2005) Part 3.

[5] S. Mitragotri et al., Immunization without needles, *Nat. Rev., Immunol.*, 5 (2005) 905-916.

[6] M. Prausnitz et al., Current status and future potential of transdermal drug delivery, *Nat. Rev. Drug Discovery*, 3 (2004) 115-124.

[7] Y.-C. Kim et al., Microneedles for drug and vaccine delivery, *Adv. Drug Deliv. Rev.*, 64 (2012) 1547-1568.

[8] X. Chen et al., Improving the reach of vaccines to low-resource regions, with a needle-free vaccine delivery device and long-term thermostabilization, *J. Control. Release,* 152 (2011) 349-344.

[9] S. T. Sanjay et al., Recent advances of controlled drug delivery using microfluidic platforms, *Adv. Drug Deliv. Rev.* (2017).

[10] H. S. Gill et al., Coated micro needles for transdermal delivery, *J. Control. Release*, 117 (2007) 227-237.

[11] P. Karande et al., Insights into synergistic interactions in binary mixtures of chemical permeation enhancers for transdermal drug delivery, *J. Control. Release*, 115 (2005) 85-93.

[12] C. M. Schoellhammer et al., Skin permeabilization for transdermal drug delivery: Recent advances and future prospects, *Expert Opin Drug Deliv.*, 11 (2014) 393-407.

[13] J. Baxter et al., Jet-induced skin puncture and its impact on needle free jet injections: Experimental studies and a predictive model, *J. Control. Release*, 106 (2005) 361-373.

[14] A. B. Baker and J. E. Sanders, Fluid mechanics analysis of a spring-loaded jet injector, *IEEE Trans. Biomed. Eng.*, 46 (1999) 235-242.

[15] J. S. Baxter et al., Jet injection into polyacrylamide gels: investigation of jet injection mechanics, *J. Biomech.*, 37 (2004) 1181-1188.

[16] J. S. Baxter et al., Needle free jet injections: Dependence of jet penetration and dispersion in the skin on jet power, *J. Control. Release*, 97 (2004) 527-535.

[17] J. P. Amorij, Needle-free influenza vaccination, *Lancet Infect. Dis.*, 10 (2010) 699-711.

[18] A. N. Zelikin et al., Materials and methods for delivery of biological drugs, *Nat. Chem.,* 8 (2016) 997-1007.

[19] P. N. Hoffman et al., A model to assess the infection potential of jet injectors used in mass immunization, *Vaccine*, 19 (2001) 4020-4027.

[20] A. Mohizin and J. K. Kim, Current engineering and clinical aspects of needle-free injectors: A review, *J. of Mechanical Science and Technology*, 32 (12) (2018) 5737-5747.

[21] J. Schramm and S. Mitragotri, Transdermal drug delivery by jet injectors: Energetics of jet formation and penetration, *Pharm. Res*., 19 (2002) 1673-1679.

[22] G. E. Theintz and P. C. Sizonenko, Risks of jet injection of insulin in children, *Eur. J. Pediatr*., 150 (1991) 554-556.

[23] S. Mitragotri, Innovation; current status and future prospects of needle free liquid jet injectors, *Nat. Rev. Drug Discov.*, 5 (2006) 543-548.

[24] U. Schneider, R. Birnbacher and E. Schober, Painfulness of needle and jet injection in children with diabetes-mellitus, *Eur. J. Pediatr.*, 153 (1994) 409-410.

[25] X. Chen, Current and future technological advances in transdermal gene delivery, *Adv. Drug Deliv. Rev*. (2017).

[26] D. O. Kane et al., Delivery of intracavernosal therapies using needle-free injection devices, *Int. J. Impot. Res.* (2017) 1-4.

[27] D. A. Fletcher and D. V. Palanker, Pulsed liquid microjet for microsurgery, *Appl. Phys. Lett*., 78 (2001) 1933-1935.

[28] D. A. Fletcher et al., Intravascular drug delivery with a pulsed liquid microjet, *Arch. Ophthalmol-Chic.*, 120 (2002) 1206-1208.

[29] J. H. Chang et al., A needle-free technique for interstitial fluid sample acquisition using a lorentz-force actuated jet injector, *J. Control. Release* (2015) 37-43.

[30] A. Arora et al., Needle-free delivery of macromolecules across the skin by nanoliter-volume pulsed microjets*, Proc. Natl. Acad. Sci. U. S. A.*, 104 (2007) 4255-4260.

[31] J. C. Stachowiak et al., Piezoelectric control of needle-free transdermal drug delivery, *J. of Controlled Release*, 124 (2007) 88-97.

[32] J. W. Waanders, *Piezoelectric Ceramics: Properties and Applications*, Chapter 5, Philips Components (1991).

[33] Physik Instrumenta, Properties of Piezo Actuators, *https://www.physikinstrumente.com/en/.*

[34] S. Takahashi, Multilayer piezoelectric ceramic actuators and their applications, *Jpn. J. Appl. Phys.* (1985) 24-41.

[35] K. Uchino, *Ferroelectric Devices*, Chapter 7, Marcel Dekker (1999).

[36] D. P. Morgan, *Surface-wave Devices for Signal Processing*, Elsevier, The Netherlands (1978).

[37] T. Higuchi, Next generation actuators leading breakthroughs, *J. of Mechanical Science and Technology*, 24 (2010) 13-18.

[38] Piezomechanik GmbH, Low voltage multilayer piezoceramic stacks, rings and chips, *Piezomechanik Product*

Catalogue (2017) 22.
[39] R. E. Newnham et al., Flextensional "Moonie" actuators, *Proceedings of 1993 IEEE Ultrasonics Symposium* (1993) 509-513.
[40] G. H. Haertling, Compositional study of PLZT rainbow ceramics for piezo actuators, *Proc. of the 9th IEEE Inte. Symp. on Applications of Ferroelectrics* (1994) 313-318.
[41] K. H. Lam et al., Lead-free piezoceramic cymbal actuator, *Sensors and Actuators A: Physical*, 125 (2006) 7.
[42] J. Ueda et al., Large effective strain piezoelectric actuators using nested cellular architecture with exponential strain amplification mechanisms, *IEEE/ASME Trans. Mechatronics*, 15 (2010) 82.
[43] J. H. Kim et al., Development of a piezoelectric actuator using a three-dimensional bridge-type hinge mechanism, *Rev. Sci. Instrum.*, 74 (2003) 24.
[44] H. J. Lee et al., Optimal design and experiment of a three-axis out-of plane nano-positioning stage using a new compact bridge-type displacement amplifier, *Rev. Sci. Instrum.*, 115103 (2015) 84.
[45] J. Jeon et al., Design and performance evaluation of a new jetting dispenser system using two piezostack actuators, *Smart Mater. Struct.,* 24 (2015) 11.
[46] M. Ling et al., Enhanced mathematical modeling of the displacement amplification ratio for piezoelectric compliant mechanisms, *Smart Mater. Struct.*, 25 (2016) 11.
[47] J. W. Gardner et al., *Microsensors, MEMS, and Smart Devices*, Chapter 10, Wiley & Sons (2001) 319-324.
[48] N. Neumann and T. Sattel, Set-oriented numerical analysis method of piezoelectrically driven non-smooth dynamical system, *IWPMA*, PA-13 (2005) 231-238.
[49] SimulationX 3.7, ESI ITI GmbH, *https://www.simulationx.com/simulation-software.html.*
[50] M. Ataei et al., Application of impulse damper in control of a chaotic friction-induced vibration, *J. of Mechanical Science and Technology*, 25 (2011) 279-285.

Mojiz Abbas Trimzi received the B.E. in chemical engineering from Dawood University of Science & Technology, Karachi, Pakistan, in 2014. In 2015, he joined Plant System & Machinery Major of University of Science and Technology (UST), Daejeon, South Korea, as integrative (M.S. leading to Ph.D.) course student. His research interests and activities as a researcher in Korea Institute of Machinery and Materials for Ph.D. include application of piezoelectric actuators in jet injectors, liquid jet dispensing heads, and displacement amplification mechanisms.

Young-Bog Ham received the M.E. and Ph.D. in mechanical engineering from Kumoh National Institute of Technology, Gumi, Korea, in 1990 and 2003. He is currently a Principal Researcher of Korea Institute of Machinery and Materials and a Professor of University of Science & Technology, Daejeon, Korea. His recent research interests and activities have included liquid dispensing application of piezoelectric actuator, design of hydrostatic transmission and water fog spray for dust suppression.

Byeung-Cheol An received the B.E. in mechanical engineering from Kyungpook National University, Daegu, South Korea in 2015, then joined Plant System & Machinery Major of University of Science and Technology (UST), Daejeon, South Korea, as integrative (M.S. leading to Ph.D.) course student. His research interests and activities include digital textile printer head design using piezoelectric actuator and cryogenic reciprocating high pressure pump design.

Jung-Ho Park received his B.S. in mechanical engineering from Chonnam National University (Korea) in 1993. He received M.S. and Ph.D. in precision machinery systems from Tokyo Institute of Technology (Japan) in 1996 and 1999, respectively. He is a Principal Researcher at Energy Systems Research Division of Korea Institute of Machinery & Materials (KIMM). His research interests include design and driving mechanism of smart actuators & sensors, functional fluids and its applications.

So-Nam Yun is a Principal Researcher of KIMM (Korea Institute of Machinery & Materials) who received the M.E. and Ph.D. in mechanical engineering all from Pukyeong National University, Busan, in 1990 and 1994. He has developed several valves with solenoid and piezo actuator. His research interests include smart actuator, valve for high-pressure hydrogen field and automatic control theory for component design.